

# A Dynamic Method to Forecast the Wheel Slip for Antilock Braking System and Its Experimental Evaluation

Yesim Oniz, *Student Member, IEEE*, Erdal Kayacan, *Student Member, IEEE*, and Okyay Kaynak, *Fellow, IEEE*

**Abstract**—The control of an antilock braking system (ABS) is a difficult problem due to its strongly nonlinear and uncertain characteristics. To overcome this difficulty, the integration of gray-system theory and sliding-mode control is proposed in this paper. This way, the prediction capabilities of the former and the robustness of the latter are combined to regulate optimal wheel slip depending on the vehicle forward velocity. The design approach described is novel, considering that a point, rather than a line, is used as the sliding control surface. The control algorithm is derived and subsequently tested on a quarter vehicle model. Encouraged by the simulation results indicating the ability to overcome the stated difficulties with fast convergence, experimental results are carried out on a laboratory setup. The results presented indicate the potential of the approach in handling difficult real-time control problems.

**Index Terms**—Antilock braking system (ABS), gray-system theory, sliding-mode control.

## I. INTRODUCTION

**A**N ANTILOCK braking system (ABS) is an electronically controlled system that helps the driver maintain control of the vehicle during emergency braking by preventing the wheels from locking up. If wheel lockup occurs, the directional stability of the vehicle will be lost, and the vehicle cannot be controlled by steering wheel inputs any longer, which may result in severe damage and injury. Hence, the primary function of ABS can be stated as to sustain stable vehicle orientation even under conditions such as sudden braking and slippery road surfaces. Another significant feature of ABS is that by keeping the brake pressure just below the point where the pressure causes a wheel to lock, the maximum braking power is ensured to stop the vehicle. This may give rise to shorter stopping distances on slippery or snowy surfaces. However, it is not possible to generalize this situation for every road type, considering that on very soft surfaces, such as gravel or unpacked snow, ABS may result in even longer stopping distances. With the increase in the amount of high-speed ground

vehicles, safety issues have become increasingly important. ABS, which was initially developed to reduce the stopping distance of airplanes, is currently one of the standard security features offered on most of the newly sold cars because of its capability to help the drivers stop the car in a shorter distance in the safest way possible.

The ABS system includes all the major components that a conventional brake system has. Additionally, it employs a hydraulic modulator, speed sensors, and an electronic control unit (ECU). The angular velocity of each wheel and the linear acceleration of the vehicle are measured with sensors. Sensors attached to the wheels send electrical pulses to the ECU at a rate proportional to the wheel speed [1]. The data are used to make the decision whether the wheel is about to lock. If a tendency toward wheel block is perceived, ECU will send signals to the hydraulic modulator, and then, the pressure in the brake cylinder will be reduced. After the wheels are prevented from locking, the pressure in the cylinder is increased again [2]. Regarding the fact that ABS can perform a cyclic application and reduction of braking force at a rate up to 15 times a second, it can be concluded that ABS is much faster and more effective than a skilled driver can be.

During accelerating or braking, friction forces that are generated between the wheel and the road surface are proportional to the normal load of the vehicle. The coefficient of this proportion is called the “road adhesion coefficient,” and it is denoted by  $\mu$ . Studies show that  $\mu$  is a nonlinear function of the wheel slip, which is defined as the measure of relative difference between the vehicle and the wheel velocities [3]. The mathematical formula for the wheel slip can be represented as

$$\lambda = \frac{V - R\omega}{V} \quad (1)$$

where  $V$  is the forward velocity of the vehicle,  $\omega$  is the angular velocity of the wheel, and  $R$  is the effective radius of the corresponding wheel. While a wheel slip of zero indicates that the wheel and vehicle velocities are the same, a ratio of one indicates that the tire is not rotating and the wheels are skidding on the road surface, i.e., the vehicle is no longer steerable.

The typical  $\mu-\lambda$  curve is obtained from the data of numerous experiments. Most of the ABS controllers are expected to keep the vehicle slip at a particular level, where the corresponding friction force (i.e., road adhesion coefficient) reaches its maximum value. Zanten *et al.* state in [4] that the wheel slip should be kept between 0.08 and 0.3 to achieve optimal performance. Furthermore, some research papers show that the reference

Manuscript received March 3, 2008; revised July 1, 2008 and September 23, 2008. This study is a follow-up to the paper titled “Simulated and Experimental Study of Antilock Braking System Using Gray Sliding Mode Control” presented in the 2007 IEEE International Conference on Systems, Man, and Cybernetics (SMC 2007), 7–10 October 2007, Montreal, Canada. This work was supported by the Scientific and Technological Research Council of Turkey (TUBITAK) under Project 107E284. This paper was recommended by Associate Editor S. X. Yang.

The authors are with the Department of Electrical and Electronics Engineering, Bogazici University, Istanbul 34342, Turkey (e-mail: yesim.oniz@boun.edu.tr; erdal.kayacan@boun.edu.tr; okyay.kaynak@boun.edu.tr).

Digital Object Identifier 10.1109/TSMCB.2008.2007966

wheel slip does not have to be a constant value. In [5], the reference wheel slip is considered a nonlinear function of some physical variables, including the velocity of the vehicle.

Although many attempts have been made over the decades, an accurate mathematical model of ABS has not been obtained yet. One of the main shortcomings is that the controller must operate at an unstable equilibrium point for optimal performance. A small perturbation of controller input may induce a drastic change in the output. Furthermore, at present, there are no affordable sensors which can accurately identify the road surface and make these data available to the ABS controller. Regarding the fact that the system parameters highly depend on the road conditions and vary over a wide range, the performance of ABS may not always be satisfactory. Moreover, sensor signals are usually highly uncertain and noisy [6].

Intelligent control algorithms, such as fuzzy-logic [7], [8], neural-network [9], and sliding-mode [10]–[16] controls, have been developed to overcome the difficulties mentioned earlier. Among others, sliding-mode control is a preferable option to regulate the wheel slip, as it guarantees the robustness of the system for changing working conditions. The main idea behind this control scheme is to restrict the motion of the system in a plane referred to as the “sliding surface,” where the predefined function of error is zero. The stability requirements for the sliding surface are described in [10]. Unlike Tan and Tomizuka [11] and Chin *et al.* [12] who assume that the optimal value of the wheel slip resulting in maximum braking torque is known, Drakunov *et al.* [13] employ sliding mode to achieve the maximum value of the friction force without the *a priori* knowledge of optimum slip. In this paper, a simplified four-wheel vehicle without lateral motion is considered, and the optimal slip is determined using a friction force observer. Kachroo and Tomizuka [14] proposed a sliding-mode controller (SMC) that can maintain the wheel slip at any desired value. They assume that the vehicle and wheel angular velocities can be obtained by direct measurement or estimation. Unsal and Kachroo [15] developed an SMC with a nonlinear observer on a quarter vehicle model to track the reference wheel slip. In this control algorithm, the nonlinear observer estimates vehicle velocity, and the controller maintains the wheel slip at the predefined value. Schinkel and Hunt [16] employ a sliding-mode-like approach for the ABS controller. To deal with the inherently nonlinear dynamics of the vehicle, two uncertain linear systems are employed.

The motivation behind this investigation is to propose an SMC coupled with a gray predictor to track the target value of the wheel slip. Although the target wheel slip is considered to be a constant corresponding to the maximum value of the road adhesion coefficient in numerous studies, it is taken to be also a velocity-dependent variable in this paper. In other words, as the velocity of the vehicle changes, the optimum value of the wheel slip will also alter. The gray predictor is employed to anticipate the future outputs of the system using current data available. It estimates the forthcoming value of both the wheel slip and the reference wheel slip; in addition, the SMC takes the necessary action to maintain the wheel slip at the desired value.

The main contributions of this paper to the existing literature are a novel strategy for the design of the sliding surface, its

integration with a gray predictor, and, finally, the experimental validation of the theoretical expectations. The main body of this paper contains six sections. In Section II, a laboratory setup of an ABS is described, and its dynamic equations are derived. The SMC and gray predictor are developed in Sections III and IV, respectively. Simulation and experimental real-time results are provided and compared in Section V. Section VI summarizes the results of this paper and discusses further possible improvements.

## II. DESCRIPTION OF EXPERIMENTAL ABS LABORATORY SETUP

Designing a controller and simulating it in the computer environment can give a general understanding about how the system may behave on an actual system; however, this information is, generally, neither sufficient nor precise. Considering unpredictable factors such as internal and external disturbances, it is possible that the system may move in an unexpected way, which makes the performance of the proposed control algorithm unacceptable. On the other hand, testing the control algorithms with real full-sized vehicles is a time- and cost-intensive process. Instead, dynamically similar test systems are used in place of actual systems to investigate system responses for different controllers.

In this paper, the ABS laboratory setup [17] manufactured by Inteco Ltd. has been used. The setup consists of two rolling wheels. The lower wheel, made of aluminum, imitates relative road motion, whereas the upper wheel, mounted to the balance lever, animates the wheel of the vehicle. In order to accelerate the lower wheel, a large flat dc motor is coupled on it. The upper wheel is equipped with a disk-brake system that is driven by a small dc motor.

Most of the ABS controllers developed aim to maintain the wheel slip at a desired value. This requires accurate measurement of the wheel slip. In this laboratory setup, the angles of rotation of the wheels are measured by two identical encoders. The accuracies of measurements are  $2\pi/2048 = 0.175^\circ$ . The angular velocities are approximated by differential quotients. The car velocity is defined to be equivalent to the angular velocity of the lower wheel multiplied by the radius of this wheel, and the angular velocity of the wheel is defined to be equivalent to the angular velocity of the upper wheel [17].

The free-body diagram of the quarter vehicle model describing longitudinal motion of the vehicle and angular motion of the wheel under braking is shown in Fig. 1. Although the model is quite simple, it preserves the fundamental characteristics of an actual system. In deriving the dynamic equations of the system, several assumptions are made. First, only the longitudinal dynamics of the vehicle are considered, i.e., the lateral and the vertical motions are neglected. Second, rolling resistance force is ignored, as it is very small due to braking. Furthermore, it is assumed that there is no interaction between the four wheels of the vehicle.

Regarding the model, there are three torques acting on the upper wheel, namely, the braking torque, the friction torque in the upper bearing, and the friction torque among the wheels. Similarly, two torques are acting on the lower wheel, namely,

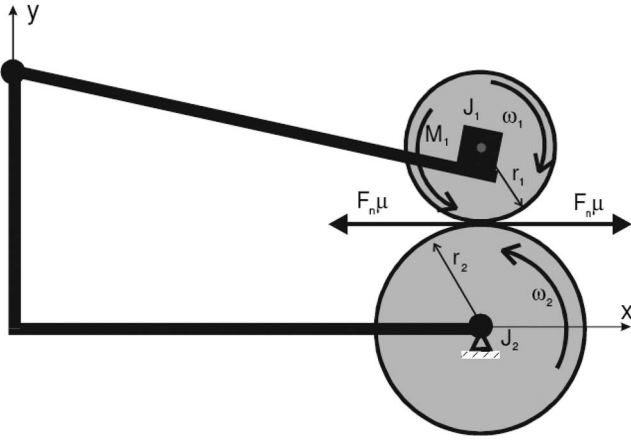


Fig. 1. Schematic view of ABS laboratory setup.

the friction torque in the lower bearing and the friction torque between these wheels.

During deceleration, a braking torque is applied to the upper wheel, which causes the wheel speed to decrease. According to Newton’s second law, the equation of the motion of the system can be written as

$$J_1 \dot{\omega}_1 = F_t r_1 - (d_1 \omega_1 + M_{10} + T_B) \quad (2)$$

$$J_2 \dot{\omega}_2 = - (F_t r_2 + d_2 \omega_2 + M_{20}). \quad (3)$$

$F_t$  in (2) and (3) stands for the road friction force which is given by the Coulomb law

$$F_t = \mu(\lambda) F_n. \quad (4)$$

$F_n$  is calculated by the following:

$$F_n = \frac{d_1 \omega_1 + M_{10} + T_B + M_g}{L (\sin \phi - \mu(\lambda) \cos \phi)} \quad (5)$$

where  $L$  is the distance between the contact point of the wheels and the rotational axis of the balance lever and  $\phi$  is the angle between the normal in the contact point and the line  $L$ .

Under normal operating conditions, the rotational velocity of the wheel would match the forward velocity of the car. When the brakes are applied, braking forces are generated at the interface between the wheel and the road surface, which causes the wheel speed to decrease. As the force at the wheel increases, slippage will occur between the tire and the road surface. The wheel speed will tend to be lower than the vehicle speed. The parameter used to specify this difference in these velocities is called wheel slip  $\lambda$  and it is defined as (Table I)

$$\lambda = \frac{r_2 \omega_2 - r_1 \omega_1}{r_2 \omega_2}. \quad (6)$$

The “road adhesion coefficient” (or coefficient of friction) is the proportion of the road friction force to the normal load of the vehicle, and it is a nonlinear function of some physical variables, including wheel slip. There are different approaches for finding the value of slip which will maximize the road adhesion coefficient and the friction force. In this paper, only two of them will be discussed and employed in the designed controllers.

TABLE I  
SYSTEM PARAMETERS

$\omega_1$	Angular velocity of the upper wheel
$\omega_2$	Angular velocity of the lower wheel
$T_B$	Braking torque
$r_1$	Radius of the upper wheel
$r_2$	Radius of the lower wheel
$J_1$	Moment of inertia of the upper wheel
$J_2$	Moment of inertia of the lower wheel
$d_1$	Viscous friction coefficient of the upper wheel
$d_2$	Viscous friction coefficient of the lower wheel
$F_n$	Total normal load
$\mu$	Road adhesion coefficient
$\lambda$	Wheel slip
$\lambda_R$	Reference slip
$F_t$	Road friction force
$M_{10}$	Static friction of the upper wheel
$M_{20}$	Static friction of the lower wheel
$M_g$	Moment of gravity acting on balance lever

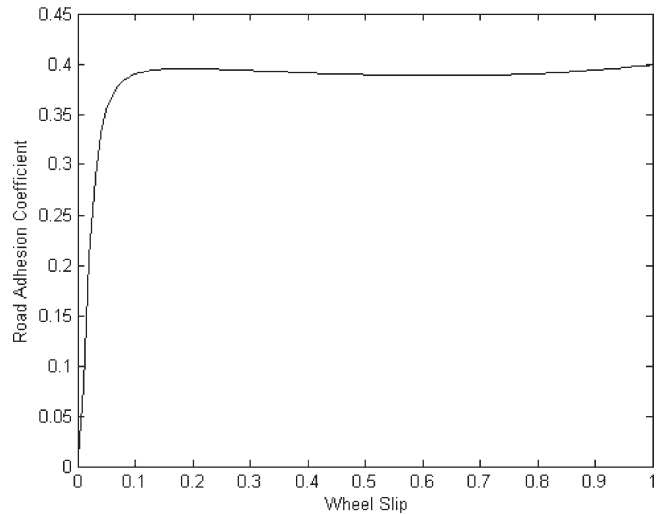


Fig. 2. Road adhesion coefficient versus wheel slip.

In the first method, it is assumed that the road adhesion coefficient is a single-variable unimodal function of the slip. The main issue in this approach is to develop a model to relate the wheel slip and the coefficient of friction to each other in such a way that the resulting graph would match with the experimental test results. Fig. 2 shows the dependence of the road adhesion coefficient to the wheel slip based on the experimental results obtained by the manufacturer of the experimental setup for one particular road condition. Based on these data, the following formula can be derived [17] to find the road adhesion coefficient corresponding to a wheel slip value:

$$\mu(\lambda) = \frac{c_4 \lambda^p}{a + \lambda^p} + c_3 \lambda^3 + c_2 \lambda^2 + c_1 \lambda. \quad (7)$$

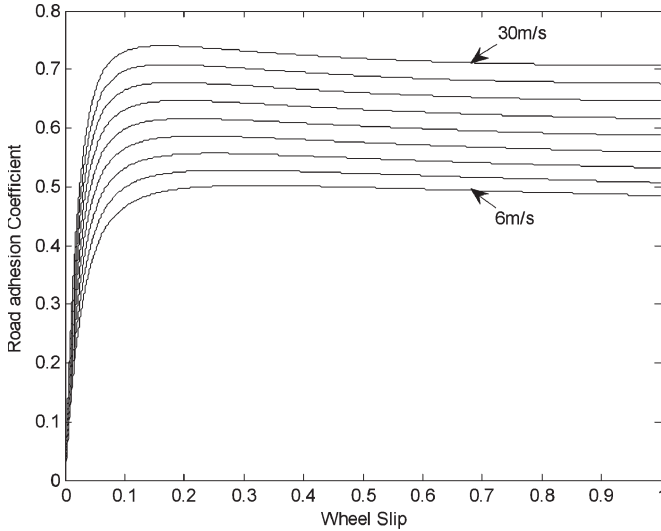


Fig. 3.  $\mu$ - $\lambda$  responses for several velocities.

Another approach followed in this paper is based on the LuGre dynamic tire/road friction model [18]. This pseudostatic model deals with the dependence of friction on velocity. The following relationship between  $\lambda$  and  $\mu$  is obtained, solving the distributed LuGre tire/road friction model [19]. The readers can refer to [20] for the numerical values used in

$$\mu(\eta, \nu) = -h(V_r) \left[ 1 + 2\gamma \frac{h(V_r)}{\sigma_0 L |\eta|} \left( e^{-\frac{\sigma_0 L |\eta|}{2h(V_r)}} - 1 \right) \right] - \sigma_2 V_r \quad (8)$$

where

$$\begin{aligned} \eta &= \frac{\lambda}{\lambda - 1} \\ h(V_r) &= \mu_c + (\mu_s - \mu_c) e^{-|V_r/V_s|^{1/2}} \\ \gamma &= 1 - \frac{\sigma_1 |\eta|}{Rwh(V_r)}. \end{aligned}$$

As can be seen from (8), if the velocity of the vehicle changes, the curve will change as well. However, the change in the curve will happen faster than a change in the vehicle velocity. Hence, it is possible to calculate the approximated peak value of the braking force produced by tire/road friction for each time step. Fig. 3 shows the relationship between  $\mu$  and  $\lambda$  for different velocities from 6 to 30 m/s for every 3-m/s increment. The results demonstrate the significant influence of velocity on the road adhesion coefficient and the corresponding slip value.

### III. DESIGN OF SMC

The vast majority of industrial applications are subjected to disturbances and parameter fluctuations because of the noise in the measurements, the mechanical stresses, and the friction, which cannot be computed or estimated beforehand. Moreover, in the derivation of the mathematical model of the plant, several assumptions and linearizations are usually made to make the calculations easier. These uncertainties can have strong adverse effects on the nonlinear control systems.

Sliding-mode control is an attractive option to solve the aforementioned problems, as it guarantees the robustness of the system for changing working conditions and modeling imprecisions [21]. A typical SMC consists of two parts. The first part guarantees the reachability of the sliding surface in finite time. The second part ensures the stability of the motion on the sliding manifold. During the sliding motion, the created sliding surface should always direct the state trajectory toward a point where a stable equilibrium point exists. This can be accomplished through the design of the sliding coefficients.

In this paper, SMC is used to track a reference wheel slip. As the main control objective is to keep the wheel slip  $\lambda$  at a desired value, it makes most sense to describe the sliding surface in terms of the error between the actual slip and its desired value. By selecting the order of differentiation  $n = 1$ , the sliding surface can be defined as [22]

$$\begin{aligned} s &= \left( \frac{d}{dt} + \delta \right)^{(n-1)} (\lambda - \lambda_R) \\ &= (\lambda - \lambda_R). \end{aligned} \quad (9)$$

The sliding motion occurs when the state  $(\lambda, \lambda_R)$  reaches the sliding surface (a point, in this case) defined by  $s = 0$ . The control that keeps the system states on the sliding surface is called the “equivalent control.” In this paper, it is called the equivalent control brake torque  $T_{b,eq}$ .

The dynamics along the sliding surface is given by

$$\dot{s} = 0. \quad (10)$$

Differentiating (9) and substituting into (10) results in

$$\dot{\lambda} = \dot{\lambda}_R. \quad (11)$$

If it is assumed that the reference wheel speed is constant, i.e.,  $\dot{\lambda}_R = 0$ , we have

$$\dot{\lambda} = 0. \quad (12)$$

Differentiating  $\lambda$  given in (6) will result in

$$\begin{aligned} \dot{\lambda} &= \frac{(\dot{\omega}_1 r_1)(\omega_2 r_2) - (\omega_1 r_1)(\dot{\omega}_2 r_2)}{(\omega_2 r_2)^2} \\ &= \frac{1}{\omega_2 r_2} \left[ -\dot{\omega}_1 r_1 + \frac{\omega_1 r_1}{\omega_2 r_2} \dot{\omega}_2 r_2 \right]. \end{aligned} \quad (13)$$

Describing the vehicle dynamics in terms of  $\dot{\omega}_1$  and  $\dot{\omega}_2$  gives

$$\dot{\omega}_1 = \frac{1}{J_1} (F_t r_1 - d_1 \omega_1 - M_{10} - T_B) \quad (14)$$

$$\dot{\omega}_2 = -\frac{1}{J_2} (F_t r_2 + d_2 \omega_2 + M_{20}). \quad (15)$$

Substituting (14) and (15) into (13) gives

$$\begin{aligned} \dot{\lambda} &= \frac{r_1}{\omega_2 r_2 J_1} (-F_t r_1 + d_1 \omega_1 + M_{10} + T_B) \\ &\quad - \frac{\omega_1 r_1}{\omega_2^2 r_2 J_2} (F_t r_2 + d_2 \omega_2 + M_{20}). \end{aligned} \quad (16)$$

Referring to (12),  $\dot{\lambda}$  stated in (16) should be zero

$$0 = \frac{r_1}{\omega_2 r_2 J_1} T_{B,\text{eq}} + \frac{r_1}{\omega_2 r_2 J_1} (-F_t r_1 + d_1 \omega_1 + M_{10}) - \frac{\omega_1 r_1}{\omega_2^2 r_2 J_2} (F_t r_2 + d_2 \omega_2 + M_{20}). \quad (17)$$

Solving for the equivalent control brake torque  $T_{b,\text{eq}}$  gives

$$T_{B,\text{eq}} = (F_t r_1 - d_1 \omega_1 - M_{10}) + \frac{\omega_1 J_1}{\omega_2 J_2} (F_t r_2 + d_2 \omega_2 + M_{20}). \quad (18)$$

Since we cannot measure the force  $F_t$  directly, it is replaced with the approximation  $\hat{F}_t$ . Then,  $\hat{T}_{B,\text{eq}}$  becomes

$$\hat{T}_{B,\text{eq}} = (\hat{F}_t r_1 - d_1 \omega_1 - M_{10}) + \frac{\omega_1 J_1}{\omega_2 J_2} (\hat{F}_t r_2 + d_2 \omega_2 + M_{20}). \quad (19)$$

If the system state  $(\lambda, \lambda_R)$  is not on the sliding surface, an additional control term called the ‘‘discontinuous control braking torque’’  $T_{b,h}$  should be added to the overall braking torque control signal. When the system state is on the sliding surface, the discontinuous control has no effect. The discontinuous control braking torque  $T_{b,h}$  is determined by the following reaching condition, where  $\eta$  is a strictly positive design parameter:

$$s \dot{s} \leq -\eta |s|. \quad (20)$$

Using (10) and (12), (20) can be rewritten, as follows:

$$s \dot{\lambda} \leq -\eta |s|. \quad (21)$$

The overall braking torque control is assumed to have the form

$$T_B = \hat{T}_{B,\text{eq}} - T_{B,h} \text{sgn}(s). \quad (22)$$

Substituting (13) into (21) and using the definition of  $T_B$  given in (22) result in the following:

$$-\frac{sr_1(\omega_2 r_1 J_2 + \omega_1 r_2 J_1)}{\omega_2^2 r_2 J_1 J_2} (F_t - \hat{F}_t) - \frac{r_1 T_{B,h}}{\omega_2 r_2 J_1} |s| \leq \eta |s|. \quad (23)$$

To ensure Lyapunov stability regardless of  $\eta$ ,  $T_{B,h}$  is chosen as

$$T_{B,h} = \frac{\omega_2 r_2 J_1}{r_1} (F + \eta). \quad (24)$$

Combining (23) and (24) gives

$$\frac{r_1(\omega_2 r_1 J_2 + \omega_1 r_2 J_1)}{\omega_2^2 r_2 J_1 J_2} |F_t - \hat{F}_t|_{\max} |s| \leq F |s|. \quad (25)$$

The function  $F$  has to be designed to ensure that the reaching condition stated in (20) will be satisfied

$$\frac{r_1(\omega_2 r_1 J_2 + \omega_1 r_2 J_1)}{\omega_2^2 r_2 J_1 J_2} |F_t - \hat{F}_t|_{\max} \leq F \quad (26)$$

where  $|F_t - \hat{F}_t|_{\max}$  is a constant corresponding to the maximum value of the estimation error.

The discontinuous switching function  $\text{sgn}(s)$  in braking torque control may give rise to the chattering phenomenon. Chattering is highly undesirable as it leads to a high number of oscillations of the system trajectory around the sliding surface and excessive load to the actuators can occur [23]. Ideally, a control strategy is required to ensure that the system dynamic is close to the sliding surface  $s(t)$ . In this investigation, a thin boundary layer neighboring the sliding surface is designed to reduce chattering. For this purpose, a continuous switching function in the form of  $s/(|s| + \delta)$ , where  $\delta \geq 0$ , is used instead of the discontinuous switching  $\text{sgn}(s)$ . The width of the boundary layer  $\delta$  has a major importance. Too wide a boundary layer may cause steady-state error, whereas too narrow a boundary layer may not eliminate the chattering completely [24].

#### IV. DESIGN OF GSMC

Time-series prediction has long been an interesting research topic, and various models, including fuzzy set theory [25], [26] and neural-network-based approaches [27], [28], have been widely used in the literature. A contemporary approach, the gray-system theory, was first proposed in 1982 [29], and the first applications appeared soon after in many different application areas [30]–[34].

Although probability and statistics, fuzzy theory, and gray-system theory all deal with uncertain information, different methods and mathematical tools are used to analyze the data. While fuzzy mathematics mainly deals with problems associated with cognitive uncertainty with the help of affiliation functions, probability and statistics need special distribution functions and samples of reasonable size to draw inferences. The methods of probability and statistics study the uncertain data from a stochastic point of view. They focus on the statistical laws existing in the history of the uncertain data and the probability of each data within possible outcomes. Serious difficulties are faced in dealing with real-time problems when no prior experience is available in fuzzy theory or when the sample size is small in statistics. Under such conditions, gray-system theory and gray controllers can provide some advantages, considering that they have the ability to handle uncertain information and use the data effectively [37]. Artificial neural networks (ANNs) or other prediction techniques can be used instead of gray predictors. However, gray predictors are generally known to be faster than ANNs.

The main advantage of gray prediction is that it requires only limited data to develop the gray model compared with the conventional controllers which need samples of reasonable size and good distribution of the data to develop an appropriate model. Gray predictors adapt their parameters to new conditions as new outputs become available. Hence, gray controllers are more robust with respect to noise, lack of modeling information, and other disturbances when compared with the conventional controllers. Consequently, the gray predictor is an excellent candidate to be incorporated in real-time control systems [35].

A gray-model first-order one variable [GM(1, 1)] type of gray model is most widely used in the literature. This model is a time-series forecasting model. The differential equations of the GM(1, 1) model have time-varying coefficients. In other

words, the model is renewed as the new data become available to the prediction model.

In order to smooth the randomness, the primitive data obtained from the system to form the GM(1, 1) are subjected to an operator named accumulating generation operator (AGO) [36]. The differential equation [i.e., GM(1, 1)], thus evolved, is solved to obtain the  $n$ -step-ahead predicted value of the system. Finally, using the predicted value, inverse AGO (IAGO) is applied to find the predicted values of the original data.

Consider a single-input single-output system. Assume that the time sequence  $X^{(0)}$  represents the outputs of the system

$$X^{(0)} = (x^{(0)}(1), x^{(0)}(2), \dots, x^{(0)}(n)), \quad n \geq 4 \quad (27)$$

where  $X^{(0)}$  is a nonnegative sequence and  $n$  is the sample size of the data. When this sequence is subjected to the AGO, the following sequence  $X^{(1)}$  is obtained, where it is obvious that  $X^{(1)}$  is monotonic increasing:

$$X^{(1)} = (x^{(1)}(1), x^{(1)}(2), \dots, x^{(1)}(n)), \quad n \geq 4 \quad (28)$$

where

$$x^{(1)}(k) = \sum_{i=1}^k x^{(0)}(i), \quad k = 1, 2, 3, \dots, n. \quad (29)$$

The generated mean sequence  $Z^{(1)}$  of  $X^{(1)}$  is defined as

$$Z^{(1)} = (z^{(1)}(1), z^{(1)}(2), \dots, z^{(1)}(n)) \quad (30)$$

where  $z^{(1)}(k)$  is the mean value of adjacent data, i.e.,

$$z^{(1)}(k) = 0.5x^{(1)}(k) + 0.5x^{(1)}(k - 1), \quad k = 2, 3, \dots, n. \quad (31)$$

The least square estimate sequence of the gray difference equation of GM(1, 1) is defined, as follows [36]:

$$x^{(0)}(k) + ax^{(1)}(k) = b. \quad (32)$$

The whitening equation is therefore as follows:

$$\frac{dx^{(1)}(t)}{dt} + ax^{(1)}(t) = b. \quad (33)$$

As shown earlier,  $[a, b]^T$  is a sequence of parameters that can be found, as follows:

$$[a, b]^T = (B^T B)^{-1} B^T Y \quad (34)$$

where

$$Y = [x^{(0)}(2), x^{(0)}(3), \dots, x^{(0)}(n)]^T \quad (35)$$

$$B = \begin{bmatrix} -z^{(1)}(2) & 1 \\ -z^{(1)}(3) & 1 \\ \vdots & \vdots \\ -z^{(1)}(n) & 1 \end{bmatrix}. \quad (36)$$

Based on (33), the solution of  $x^{(1)}(t)$  at time  $k$  is

$$x_p^{(1)}(k + 1) = \left[ x^{(0)}(1) - \frac{b}{a} \right] e^{-ak} + \frac{b}{a}. \quad (37)$$

To obtain the predicted value of the primitive data at time  $(k + 1)$ , the IAGO is used to establish the following gray model:

$$x_p^{(0)}(k + 1) = \left[ x^{(0)}(1) - \frac{b}{a} \right] e^{-ak} (1 - e^a) \quad (38)$$

and the predicted value of the primitive data at time  $(k + H)$

$$x_p^{(0)}(k + H) = \left[ x^{(0)}(1) - \frac{b}{a} \right] e^{-a(k+H-1)} (1 - e^a). \quad (39)$$

The parameter  $(-a)$  in the GM(1, 1) model is called the “development coefficient,” which reflects the development states of  $X_p^{(1)}$  and  $X_p^{(0)}$ . The parameter  $b$  is called the “gray action quantity,” which reflects changes contained in the data because of being derived from the background values [37].

Gray-system theory is distinguished with its ability to deal with systems that have partially unknown parameters. It is therefore a good candidate for use in real-time control systems. With the use of gray-system mathematics (for instance, gray equations, gray matrices, etc.), it is possible to generate meaningful information using insufficient and poor data. Gray predictors have the ability to predict the future outputs of a system by using recently obtained data. On the other hand, SMC is known by its robustness. The combination of gray predictors with conventional SMC is therefore likely to result in an increase in the performance specifications (i.e., overshoot, settling time, etc.) as such a controller would anticipate the upcoming values of the wheel slip, all the while ensuring robustness to varying dynamic conditions. This idea has been investigated in the literature earlier [38], with the design of the gray SMC (GSMC) controller being based on a sliding surface which is a line. In this paper, a simpler approach is proposed, defining the time-varying gray sliding surface  $s(\lambda; t)$  as a point, as indicated in the following:

$$s(\lambda, t) = (e + e_p) \quad (40)$$

where  $e$  is the system error,  $e_p = \lambda_R - \lambda_p$  is a value predicted by the GM(1, 1) model, and  $\lambda_p$  is the predicted value of the wheel slip. If the Lyapunov candidate function  $V_L$  is defined as

$$V_L = \frac{1}{2} (s(\lambda, t))^2 \quad (41)$$

then it is guaranteed that the tracking error of GSMC will be less than one of the conventional SMC [38]. The structure of the proposed GSMC is shown in Fig. 4. The wheel slip is the input for the controller. The gray predictor estimates the forthcoming values of the wheel slip using its current and preceding values. With the information on the future values of the wheel slip, it is reasonable to expect that SMC can control the system more effectively.

The required minimum number of data points to form a gray model is four. However, there are no strict rules for determining

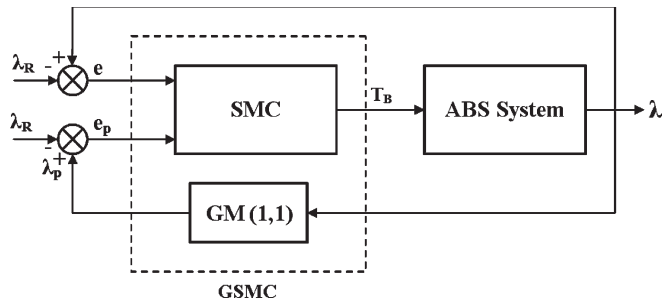


Fig. 4. Structure of GSMC.

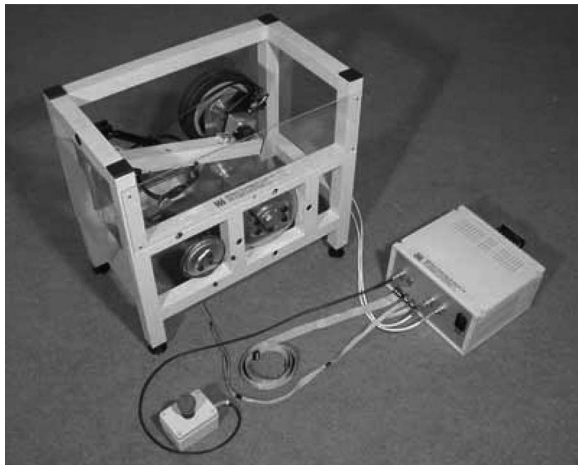


Fig. 5. ABS laboratory setup.

the prediction window size. In this paper, five data points are employed to forecast the forthcoming values of the wheel slip. It is still an open question of how to select the optimum number of data points for gray modeling [39].

## V. SIMULATED AND EXPERIMENTAL RESULTS

To investigate the performance of the proposed controllers, a number of computer-simulated dynamic responses are obtained. Furthermore, the simulated designs are built and used in the real-time experiments on the dynamic test stand. All figures that follow show simulation and experimental results for a car with the initial longitudinal velocity  $V = 70$  km/h maneuvering on a straight line (Fig. 5). Two approaches are followed to determine the reference wheel slip value. In the first case, in accordance with the basic assumption made (12) in the derivation of the SMC, the reference wheel slip is taken to be constant ( $\lambda = 0.2$ ). In the second case, in order to check the performance of this controller under varying slip conditions, the reference slip is considered to vary as a function of the vehicle velocity. For this purpose, a pseudostatic curve is used to calculate the reference wheel slip and the corresponding tire friction coefficient. These values are used to construct a table, which relates the vehicle speed to the peak values of tire road friction coefficient and to the reference wheel slip. Next, the reference wheel slip is made available to the proposed controller at each step of the control loop. All tests are run for a 1-ms sampling period [20].

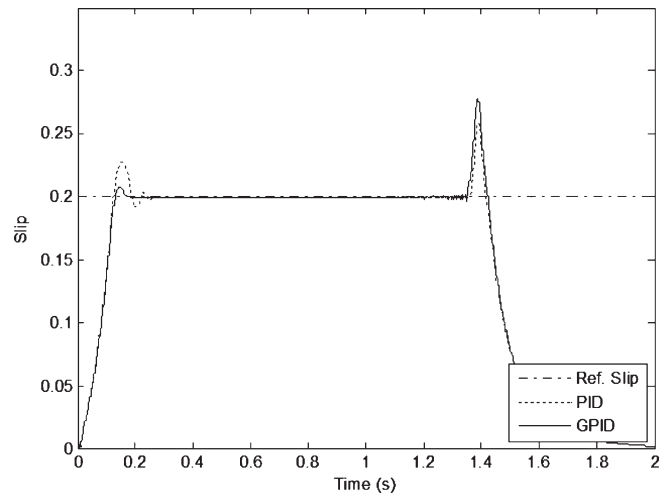


Fig. 6. Wheel slip of PID and GPID for a constant reference.

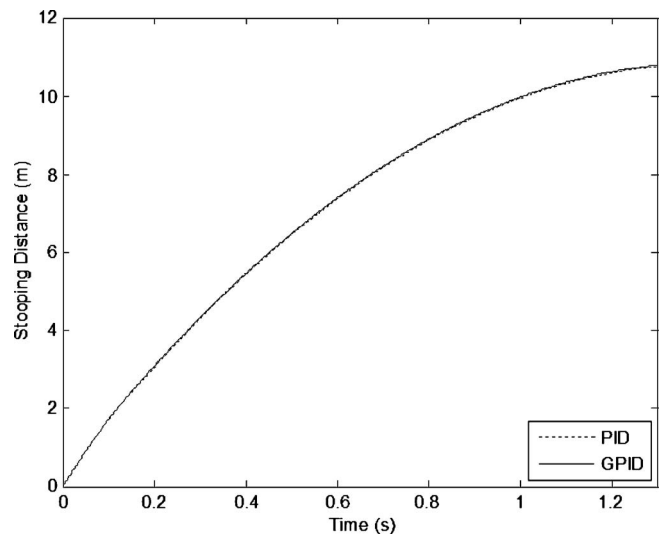


Fig. 7. Stopping distance of PID and GPID for a constant reference.

### A. Simulated Results

In Figs. 6 and 7, the responses of the model to a PID controller and to a gray PID (GPID) controller are compared. The PID controller gains are selected as  $K_P = 500$ ,  $K_I = 15$ , and  $K_D = 2$ . The stopping distance for both controllers are similar. It can be inferred from Fig. 6 that GPID controller results in faster convergence to the reference values and smaller overshoot. Furthermore, it causes the system to have less fluctuations. It is to be noted that in practice, there would be a relay-type switch in the braking system of the vehicle. When the velocity of the vehicle decreases below a minimum value, the ABS controller is switched off, and the regular brakes are applied. This means that the last portion of the simulation curve when the slip value changes from the reference value would not be seen, the maximum braking torque being applied to the wheels without considering the target value of slip.

Fig. 8 shows system responses of SMC and SMC coupled to a gray predictor for a constant reference wheel slip of  $\lambda = 0.2$ . The step size of GSMC is taken to be ten, based on some

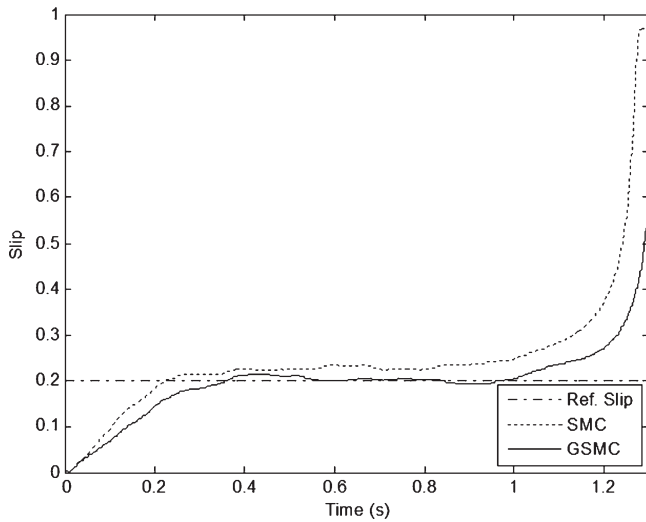


Fig. 8. Wheel slip of SMC and GSMC for a constant reference.

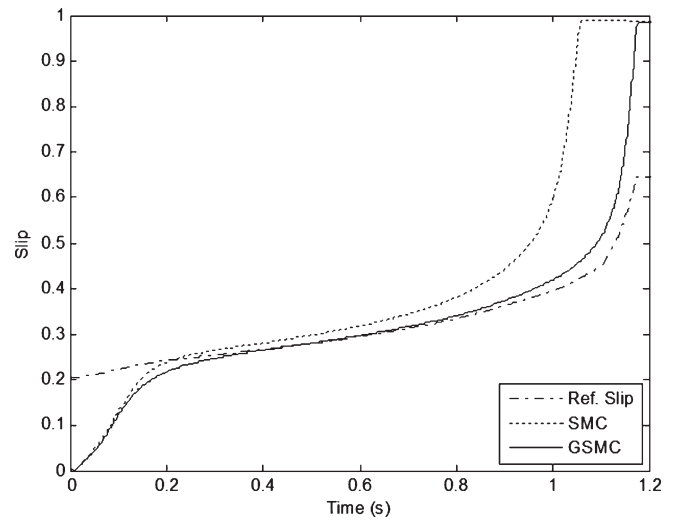


Fig. 10. Wheel slip of SMC and GSMC for velocity-dependent reference.

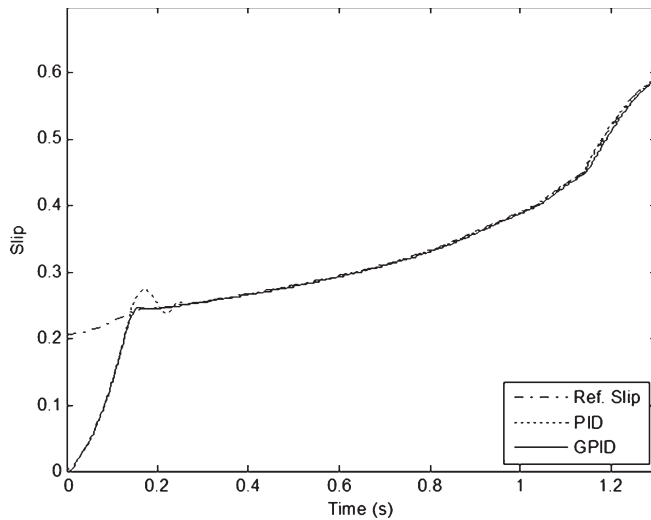


Fig. 9. Wheel slip of PID and GPID for velocity-dependent reference.

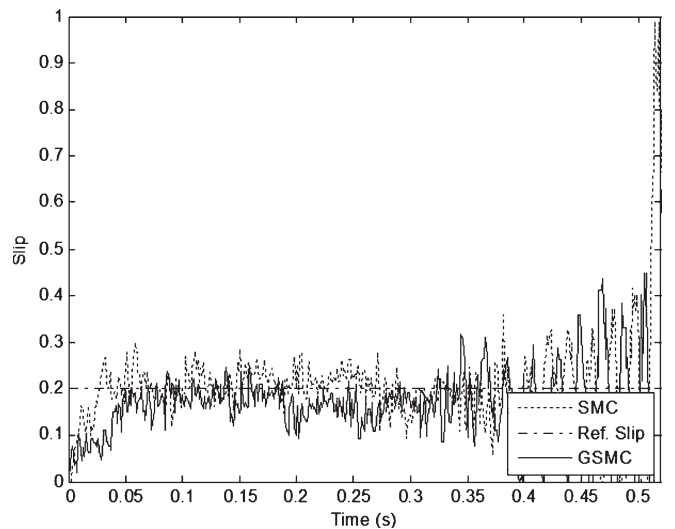


Fig. 11. Wheel slip of SMC and GSMC for constant reference.

trials for better performance. In order to simulate more realistic real-life conditions, a band-limited white noise is added to the system at slip measurements. The numerical values of noise power and the design parameters  $\eta$  and  $\delta$  are selected as  $1 \times 10^{-5}$ , 1.2 and 0.2, respectively. Although both controllers possess steady-state errors, GSMC exhibits better performance when compared with the conventional SMC. Stopping distance values are approximately the same as the values obtained for PID and GPID; hence, they are not presented here. Fig. 9 shows the simulation results of PID and GPID controllers for velocity-dependent reference wheel slip using the formula presented in [5]. In a similar manner, the system responses of SMC and GSMC are shown in Fig. 10. Regarding the simulation results, it can be inferred that all controllers are capable of tracking the reference wheel slip satisfactorily. Similar to the previous case, the steady-state error in GSMC is less than that in conventional SMC, and faster convergence and smaller overshoot are observed for GPID compared with PID. However, no drastic change in stopping distances is seen.

### B. Experimental Results

A series of experiments have been conducted to determine the performance of the proposed controller for different cases and conditions. For the experiments, the ABS setup of Inteco Ltd. is used [17]. To imitate the behavior of the vehicle during braking on a dry and straight road, the wheel is accelerated until the velocity of the wheel reaches 70 km/h. Once it reaches the velocity limit, the braking operation is started. There is another velocity threshold which states the minimum velocity level for applying ABS control algorithms. Under this minimum value of the velocity, the system becomes unstable if the ABS algorithm is applied. Under such a circumstance, the maximum braking torque should be applied to the wheels, without considering the target value of slip.

One of the parameters that has a deep impact on the effectiveness of the controller is the step size of the gray predictor. The step size should be selected appropriately, since a large step size may result in a slow system response, whereas a small step size may cause overshoots. In the experiments, the step size of GSMC is set to ten. Figs. 11 and 12 show the

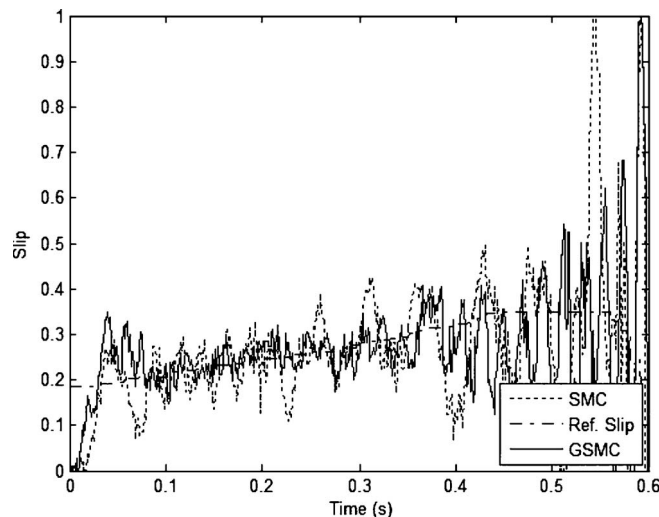


Fig. 12. Wheel slip of SMC and GSMC for velocity-dependent reference.

system responses for constant and velocity-dependent reference wheel slip values, respectively. Although the response of SMC is acceptable, the results of the experiments indicate that gray predictive controllers are robust in real-time systems that are subjected to noise from both inside and outside the system.

## VI. CONCLUSION

As has been stated earlier, gray-system theory is distinguished with its ability to deal with the systems that have partially unknown parameters. Gray predictors have the ability to predict the future outputs of a system on the basis of recently obtained data, albeit it may be insufficient and poor. On the other hand, SMCs are known for their robustness. It is therefore reasonable to expect that the combination of gray predictors with conventional SMCs will be capable of alleviating the problems met in the real-time control of systems with uncertain and time varying dynamics, resulting in an increase in the performance specifications, e.g., the amount of overshoot, settling time, etc. In the case of the control of an ABS, such a controller would anticipate the upcoming values of the wheel slip while ensuring robustness to varying dynamic conditions. This is the motivation behind this paper. In this paper, a novel gray sliding-mode control algorithm is proposed, and its formulation for the control of an ABS system is derived and subsequently tested on a quarter vehicle model. Four different controllers, namely a PID, a PID coupled with a gray predictor, a conventional SMC, and a conventional SMC with a gray predictor, are simulated on a quarter vehicle model and compared. The findings indicate that the coupling of a gray predictor with a PID- or SMC-based approach results in less steady-state error, less overshoot and better noise response. From an implementation point of view, the use of GSMC is preferable to GPID since the former is a model-free approach. Encouraged by these results, a series of experimental studies are carried out on a laboratory setup for both constant and velocity-dependent reference wheel slip values. When the performances of the conventional SMC and GSMC are compared, it is seen that the results are in accordance with the expectations obtained from the simulation studies, with

the latter displaying a better noise response. In conclusion, it can be stated that the controller proposed in this paper is capable of handling difficult real-time control problems. Further experimental investigations are in progress for different road conditions and for selecting the step size of the gray predictor adaptively.

## REFERENCES

- [1] The Maintenance Council of the American Trucking Associations, *Technician Guidelines for Antilock Braking Systems*, 1998. Publication No. FHWA-MC-98-008.
- [2] Y. T. Hattori, T. Takahashi, and A. Tanaka, "An application of the adaptive method for the sliding mode control of the brake system," in *Proc. Int. Symp. Adv. Veh. Control*, Nagoya, Japan, 1998, pp. 611–616.
- [3] A. Harifi, A. Aghagolzadeh, G. Alizadeh, and M. Sadeghi, "Designing a sliding mode controller for antilock brake system," in *Proc. Int. Conf. Comput. Tool*, Serbia and Montenegro, Europe, 2005, pp. 611–616.
- [4] A. Zanten, R. Erhardt, and A. Lutz, "Measurement and simulation of transients in longitudinal and lateral tire forces," *SAE Transact.*, vol. 99, no. 6, pp. 300–318, 1990. Paper 900210.
- [5] J. Svendenius, *The Tire Models for Use in Braking Applications*. Lund, Sweden: Dept. Autom. Control, Lund Inst. Technol., 2003.
- [6] M. R. Akbarzadeh, K. J. Emami, and N. Pariz, "Adaptive discrete-time fuzzy sliding mode control for anti-lock braking systems," in *Proc. Annu. Meeting North Amer.*, New Orleans, LA, 2002, pp. 554–559.
- [7] C. M. Lin and C. F. Hsu, "Self-learning fuzzy sliding-mode control for antilock braking systems," *IEEE Trans. Control Syst. Technol.*, vol. 11, no. 2, pp. 273–278, Mar. 2003.
- [8] W. Y. Wang, K. C. Hsu, T. T. Lee, and G. M. Chen, "Robust sliding mode-like fuzzy logic control for anti-lock braking systems with uncertainties and disturbances," in *Proc. Int. Conf. Mach. Learn. Cybern.*, Taipei, Taiwan, 2003, vol. 1, pp. 633–638.
- [9] C. M. Lin and C. F. Hsu, "Neural-network hybrid control for antilock braking systems," *IEEE Trans. Neural Netw.*, vol. 14, no. 2, pp. 351–359, Mar. 2003.
- [10] W. C. Lin and Y. K. Chin, "Variable-structure brake control for anti-skid and anti-spin," General Motors Res. Lab., Warren, MI, Rep. EG-275, 1986.
- [11] H. S. Tan and M. Tomizuka, "An adaptive and robust vehicle traction controller design," in *Proc. Amer. Control Conf.*, Pittsburgh, PA, 1989, pp. 1053–1058.
- [12] Y. K. Chin, W. C. Lin, D. M. Sidlosky, and M. S. Sparschu, "Sliding-mode ABS wheel slip control," in *Proc. Amer. Control Conf.*, Chicago, IL, 1992, pp. 1–6.
- [13] S. Drakunov, U. Ozguner, P. Dix, and B. Ashrafi, "ABS control using optimum search via sliding modes," *IEEE Trans. Control Syst. Technol.*, vol. 3, no. 1, pp. 79–85, Mar. 1995.
- [14] P. Kachroo and M. Tomizuka, "Sliding mode control with chattering reduction and error convergence for a class of discrete nonlinear systems with application to vehicle control," in *Proc. ASME Meeting Int. Mech. Eng. Congr. Expo.*, 1995, pp. 225–233. DSC-Vol. 57-1.
- [15] C. Unsal and P. Kachroo, "Sliding mode measurement feedback control for antilock braking systems," *IEEE Trans. Control Syst. Technol.*, vol. 7, no. 2, pp. 271–281, Mar. 1999.
- [16] M. Schinkel and K. Hunt, "Anti-lock braking control using a sliding mode approach," in *Proc. Amer. Control Conf.*, Anchorage, AK, 2002, pp. 2386–2391.
- [17] "User's manual," *The Laboratory Antilock Braking System Controlled from PC*, Inteco Ltd., Crakow, Poland, 2006.
- [18] H. Olsson, "Control systems with friction," Ph.D. dissertation, Lund Inst. Technol., Lund, Sweden, 1996.
- [19] J. Yi, L. Alvarez, R. Horowitz, and C. Canudas, "Adaptive emergency braking control based on a tire/road friction dynamic model," in *Proc. 39th Conf. Decision Control*, Sydney, Australia, 2000, vol. 1, pp. 456–461.
- [20] Y. Oniz, E. Kayacan, and O. Kaynak, "Simulated and experimental study of antilock braking system using gray sliding mode control," in *Proc. IEEE Int. Conf. Syst., Man Cybern.*, Montreal, QC, Canada, 2007, pp. 90–95.
- [21] V. Utkin, J. Guldner, and J. Shi, *Sliding Mode Control in Electromechanical Systems*. Philadelphia, PA: Taylor & Francis, 1999.
- [22] K. R. Buckholtz, "Reference input wheel slip tracking using sliding mode control," presented at the SAE 2002 World Congr., Detroit, MI, 2002, Paper No. 2002-01-0301.

- [23] C. Edwards and S. K. Spurgeon, *Sliding Mode Control Theory and Applications*. New York: Taylor & Francis, 1998.
- [24] Y. J. Huang, T. C. Kuo, and S. H. Chang, "Adaptive sliding-mode control for nonlinear systems with uncertain parameters," *IEEE Trans. Syst., Man, Cybern. B, Cybern.*, vol. 38, no. 2, pp. 534–539, Apr. 2008.
- [25] S. M. Chen and J. R. Hwang, "Temperature prediction using fuzzy time series," *IEEE Trans. Syst., Man, Cybern. B, Cybern.*, vol. 30, no. 2, pp. 263–275, Apr. 2000.
- [26] K. Huang and H. K. Yu, "Ratio-based lengths of intervals to improve fuzzy time series forecasting," *IEEE Trans. Syst., Man, Cybern. B, Cybern.*, vol. 36, no. 2, pp. 328–340, Apr. 2006.
- [27] S. Narayan, G. A. Tagliarini, and E. W. Page, "Enhancing MLP networks using a distributed data representation," *IEEE Trans. Syst., Man, Cybern. B, Cybern.*, vol. 26, no. 1, pp. 143–149, Feb. 1996.
- [28] C. L. P. Chen and J. Z. Wan, "A rapid learning and dynamic stepwise updating algorithm for flat neural networks and the application to time-series prediction," *IEEE Trans. Syst., Man, Cybern. B, Cybern.*, vol. 29, no. 1, pp. 62–72, Feb. 1999.
- [29] J. L. Deng, "Control problems of gray system," *Syst. Control Lett.*, vol. 1, no. 5, pp. 288–294, 1982.
- [30] B. Cheng, "The gray control on industrial process," *J. Huangshi College*, vol. 1, pp. 11–23, 1986.
- [31] J. J. Luo and B. X. Zhang, "A study of gray forecasting and its control analysis of grain yield," *J. Grey Syst.*, vol. 1, no. 1, pp. 91–98, 1989.
- [32] Y. Tamura, D. P. Zhang, U. Umeda, and K. Sakashit, "Load forecasting using gray dynamic model," *J. Grey Syst.*, vol. 4, no. 1, pp. 45–48, 1992.
- [33] S. Y. Song, "The application of gray system theory to earthquake prediction in Jiangsu area," *J. Grey Syst.*, vol. 4, no. 4, pp. 359–367, 1992.
- [34] C. M. Hong, S. C. Lin, and C. T. Chiang, "Control of dynamic systems by fuzzy-based gray prediction controller," *J. Grey Syst.*, vol. 7, no. 1, pp. 23–44, 1995.
- [35] E. Kayacan and O. Kaynak, "An adaptive gray fuzzy PID controller with variable prediction horizon," in *Proc. SCIS&ISIS*, Tokyo, Japan, 2006, pp. 760–765.
- [36] J. L. Deng, "Introduction to gray system theory," *J. Grey Syst.*, vol. 1, no. 1, pp. 1–24, 1989.
- [37] S. F. Liu and Y. Lin, *An Introduction to Grey Systems*. Grove City, PA: IIGSS Academic Publisher, 1998.
- [38] H. C. Lu, "Grey prediction approach for designing gray sliding mode controller," in *Proc. IEEE Int. Conf. Syst., Man Cybern.*, The Hague, The Netherlands, 2004, pp. 403–408.
- [39] Y. P. Huang and T. M. Yu, "The hybrid gray-based models for temperature prediction," *IEEE Trans. Syst., Man, Cybern. B, Cybern.*, vol. 27, no. 2, pp. 284–292, Apr. 1997.



**Yesim Oniz** (S'06) was born in Istanbul, Turkey, on July 10, 1981. She received the B.Sc. degree in mechatronics engineering from Sabanci University, Istanbul, in 2004 and the M.Sc. degree in electrical and electronic engineering from Bogazici University, Istanbul, in 2007, where she is currently working toward the Ph.D. degree in electrical and electronic engineering in the Department of Electrical and Electronics Engineering.

She is currently a Research Assistant with the Mechatronics Research and Application Center, Department of Electrical and Electronics Engineering, Bogazici University. Her research interests include robotics, variable structure systems, intelligent control, and fuzzy and neurofuzzy controls.



**Erdal Kayacan** (S'06) was born in Istanbul, Turkey, on January 7, 1980. He received the B.Sc. degree in electrical engineering from Istanbul Technical University, Istanbul, in 2003 and the M.Sc. degree in systems and control engineering from Bogazici University, Istanbul, in 2006, where he is currently working toward the Ph.D. degree in electrical and electronic engineering in the Department of Electrical and Electronics Engineering.

He is currently a Research Assistant with the Mechatronics Research and Application Center, Department of Electrical and Electronics Engineering, Bogazici University. His research interests include soft computing, intelligent control, fuzzy theory, gray-system theory, analysis and control of electrical machines, and harmonizing international standards related to electric machines and drives.



**Okyay Kaynak** (SM'90–F'03) received the B.Sc. (First Class Honors) and the Ph.D. degrees in electronic and electrical engineering from the University of Birmingham, Birmingham, U.K., in 1969 and 1972, respectively.

From 1972 to 1979, he held various positions within the industry. Since 1979, he has been the Department of Electrical and Electronics Engineering, Bogazici University, Istanbul, Turkey, where he is currently a Full Professor. With Bogazici University, he was the Chairman of the Department of Computer Engineering and of the Department of Electrical and Electronic Engineering and was the Director of the Biomedical Engineering Institute; currently, he is the United Nations Educational, Scientific, and Cultural Organization Chair on Mechatronics and the Director of the Mechatronics Research and Application Center. He was a long-term (near to or more than a year) Visiting Professor/Scholar with various institutions in Japan, Germany, the U.S., and Singapore. He has authored three books and edited five and authored or coauthored more than 200 papers that have appeared in various journals and conference proceedings. He is on the editorial or advisory boards of a number of scholarly journals. His current research interests include intelligent control and mechatronics.

Dr. Kaynak served as the President of the IEEE Industrial Electronics Society (2002–2003) and as an Associate Editor of the IEEE TRANSACTIONS ON INDUSTRIAL ELECTRONICS and the IEEE TRANSACTIONS ON NEURAL NETWORKS. He is currently the Editor-in-Chief of the IEEE TRANSACTIONS ON INDUSTRIAL INFORMATICS.